



Cement-based mixes: Shearing properties and pore pressure

Thibaut Lecompte ^a, Arnaud Perrot ^{a,*}, Vincent Picandet ^a, Hervé Bellegou ^a, Sofiane Amziane ^b

^a Laboratoire d'ingénierie des Matériaux de Bretagne, Université de Bretagne Sud, Université Européenne de Bretagne - Centre de Recherche de Saint Maudé, BP 92116, 56321 Lorient Cedex, France

^b Clermont Université, Université Blaise Pascal, EA 3867, Laboratoire de Mécanique et Ingénieries, BP 10448, F-63000 Clermont-Ferrand, France

ARTICLE INFO

Article history:

Received 8 April 2011

Accepted 14 September 2011

Keywords:

Rheology (A)

Fresh concrete (A)

Workability (A)

Thixotropy

ABSTRACT

This study presents original results on the rheological measurement of concrete mixes. It focuses on how to determine their mechanical and physical behavior under shearing stress. More specifically, the influence of aggregate content on shearing properties is studied. A vane rheometer was developed to characterize fresh cement-based materials. In addition to the conventional concrete rheometer, a special hydraulic pressure transducer was fitted to the container to monitor the pore water pressure variation while shearing the material. Experiments on cement paste, mortar, and concrete bring a new approach to help us understand the behavior of fresh-state mixes. The results show 1) a correlation between water pore pressure and torque applied on the vane; 2) a critical sand volume fraction, ϕ_c , as a limit between colloidal interaction behavior and frictional behavior in mortars; beyond this critical fraction, a leap in yield stress and a drop in pore pressure due to granular dilatancy are noticed; 3) the granular content clearly influences the increase in yield stress of the cement mixes: above ϕ_c , this increase becomes negligible.

© 2011 Elsevier Ltd. All rights reserved.

1. Introduction

The emergence of several more complex concrete mixtures, such as self compacting concrete (SCC), has caused concrete rheology to become paramount [1].

Cement-based mixes are suspensions of particles in a wide range of sizes. It has been demonstrated that the mechanisms governing the material's shearing properties strongly depend on particle size and volume fraction.

Coussot and Ancey [2] define a classification of the rheophysical regimes of suspensions. At a low strain rate, they distinguish three successive paramount effects depending on the suspension solid volume fraction and particle size: Brownian effects for highly-dilute suspensions, colloidal effects for “soft” suspensions, and friction effects for “hard” suspensions. The transition between frictional and hydrodynamic interactions occurs for a critical value of solid particles volume fraction ϕ_c . Considering a suspension of aggregates in a cement paste, Yammine et al. [3] clearly show that this transition induces a leap in yield stress. The critical volume fraction ϕ_c is the lower value of the solid fraction which allows particle contact networks to exist throughout the suspension. Then, below this value, the cement paste forms layers between particles and controls the yielding process.

Mansoutre et al. [4] demonstrate for C_3S paste that above a critical concentration ϕ_c of C_3S particles, normal forces appear during shearing in common rotational plate–plate geometry. The appearance of

normal forces proves the existence of particles contact and sample volume increase. At such a volume fraction, a C_3S paste behaves in part as a dense dilatative granular material [4,5]. Such behavior is also reported for cement pastes [6].

Above ϕ_c , contact throughout the suspension forms a continuous network of particles. Yielding is then strongly influenced by granular friction. Abriak and Caron [7] show that for such a packing, shearing consists in the formation of voids, and consequently in the concentration of local forces in a localized yield band. It gives a new resistance to the medium and induces dilatancy. Stone and Muir Wood [8] observe that particle size affects the thickness of localization, and consequently influences both dilatancy (void creation) and yield behavior of granular media. Void creation induces pore pressure variations that can be representative of the material's dilatant behavior. Amziane et al. experimentally show that pore pressure and yield stress variations are linked [9,10]. Their work showed that before the Vicat initial setting time, the pore pressure decrease seemed to be proportional to the yield stress increase.

Usually, the dilatancy of granular media can be measured with a triaxial device or with a shear box. In the shear box device, two displacement sensors are placed at both ends of the box to quantify the dilatancy. For the triaxial method, pore pressure variation is the parameter used to quantify the volume variation of the specimen under shearing.

These two experimental techniques are inappropriate in the case of fresh cement-based material, due to the high fluidity of the material, the range of applied shear rate and the representative volume required for a representative test.

Several concrete rheometers have been developed in the last three decades [11,12]. In the case of concentrated suspensions, such as fresh cement-based mixtures, the vane geometry allows for an accurate and

* Corresponding author. Tel.: +33 297874577; fax: +33 297874571.

E-mail address: arnaud.perrot@univ-ubs.fr (A. Perrot).

direct measurement of yield stress [13–17]. Recent studies on fresh cement-based mixes show that yield stress is the most influential parameter for concrete casting and pre-casting [18–21]. With vane geometry, the stress growth test is able to measure the yield stress [22], which is generally regarded as the transition stress between elasto-plastic solid-like behavior and viscous liquid-like behavior.

The main objective of this work is to describe the transition in shearing regime for cement mixes according to aggregates content and setting time (during the first 3 h). To reach this goal, dilatancy and yield stress have to be estimated for several aggregate contents (from no aggregate to aggregate packing) and resting times. Therefore, an innovative rheometer has been developed to measure simultaneously shearing torque and pore pressure at the container wall.

The present work begins with a study performed on self-compacting cement-based mixes, to observe the influence of sand, gravel, and paste age. This study helps validate the use of such a device, and makes some recommendations. The second part focuses on the influence of sand volume fraction (aggregate content) on yield stress, structural build-up, and the drop in pressure properties.

2. Experimental procedures

2.1. Materials

The different mix designs are presented in Table 1.

A Portland cement (CEM I/52.5 N) is used. According to the manufacturer, the cement is 95.5% clinker (in mass fraction) and 4% gypsum. The cement has no other mineral admixture or filler. The cement size distribution, measured in ethanol using a laser granulometer, ranges between 1 μm and 100 μm and the d_{50} is 15 μm .

For self-compacting concrete (SCC), common Loire river sand was used. Sand particle size ranges from 20 μm to 3.15 mm and sand absorption capacity is 0.9%. Gravels were 6 mm to 10 mm crushed gravels, with an absorption capacity of 3.6%. The filler is a limestone, with particle sizes ranging from 0.1 to 100 μm (d_{50} = 15 μm). The amount of water is corrected to take into account the water absorbed by sand and gravels. It ensures that the cement paste presents a constant water to cement ratio, W/C, equal to 0.35.

The self-compacting cement paste (SCP) is also tested without any aggregate.

For mortar mixes M_0 to M_3 , French normalized sand (CECN EN 196-1) was used to reduce the variability of size distribution between the samples. This sand has a water absorption capacity of 0.9% in mass. The

Table 2
Vane geometries.

	Radius (mm)	Height (mm)	Stress range (Pa)
T_1	20	44	100–5000
T_2	40	60	10–500

amount of water is also corrected to take into account the water absorbed by the sand. It ensures that the cement paste presents a constant water to cement ratio, W/C, equal to 0.3 for all mortars.

For all mixes, a water-reducing admixture is used. It is a polycarboxylate-based superplasticizer, a liquid containing 20% of dry extract. Its recommended dosage ranges from 0.3% to 3% per weight of cement.

The standard French normalized sand used for mortar mixes was also tested in saturated condition. The sand volume fraction of the sheared sample was 0.65.

2.2. Device

Two different rheometers were used. The first, called device 1, is a conventional Anton Paar Rheolab QC rheometer equipped with a vane geometry, well adapted for cement paste and mortar. The vane geometry used in this study consisted of four blades around a cylindrical shaft. The blade height and diameter were chosen from two tool geometries to optimize the measurement accuracy. Tool geometries are summarized in Table 2 with the ranges of associated measured yield stress. This device was used to measure the increase in yield stress of the material at rest.

The second, called device 2, is an original rheometer fitted with pressure transducers. It was designed as depicted in Fig. 1. This rheometer consists of a four-blade vane, immersed in the granular fluid suspension and rotating at a controlled rate. The vane dimensions are quite large, so as to enable the study of concrete mixes: 120 mm height H , and 120 mm diameter D . The vane is connected to the rheometer with a keyless chuck. The rheometer can be quickly set on a framework and positioned in a standard container to facilitate test operation and ensure consistent test geometry (Fig. 1). The gap between blades and container wall is always greater than ten times the biggest particle size, in order to avoid granular effects such as arch formation or premature localization on the container wall. In the present study, two containers were used: a 186 mm (inner-diameter) cylinder for cement pastes or mortars, and a

Table 1
Mix designs and performed tests.

	Type of sand	Cement (kg/m ³)	Water	Filler	Admixture	Sand	Gravel	W/C (taking into account aggregates water absorption)	Tested on device 1	Tested on device 2
SCP	Loire river sand	C = 874	0.35 C	0.781 C	1.42% C			0.35	×	×
SCC		C = 320	0.425 C			2 C	3 C			×
Saturated sand	French Normalized sand		350			1755			×	×
M_0		C = 1606	0.3 C		2.5% C			0.3	×	×
M_1		C = 1227	0.305 C			C			×	×
$M_{1.5}$		C = 993	0.309 C			1.5 C			×	×
$M_{1.75}$		C = 834	0.314 C			1.75 C			×	×
$M_{1.88}$		C = 772	0.316 C			1.88 C			×	
M_2		C = 744	0.317 C			2 C			×	×
$M_{2.5}$		C = 718	0.318 C			2.5 C			×	×
M_3		C = 631	0.323 C			3 C			×	

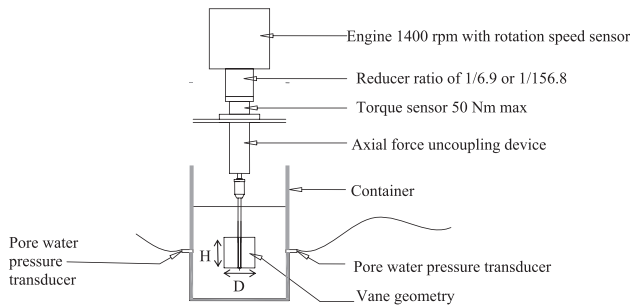


Fig. 1. Rheometer fitted with pressure sensors.

500 mm (inner-diameter) cylinder for concretes. The inner surfaces of the containers were covered with sandpaper to avoid slippage.

The pore pressure is measured along the container wall using a pressure transducer device (see “1” in Fig. 2) through the “de-aerator block” filled with water (“2” in Fig. 2). To separate the cement paste from the measurement system, a filtering device (compacted cotton fibers) was used (“3” in Fig. 2). The balance of pressure between the water in the chamber and the water in the paste was achieved by the transfer of pressure through the filter. Tests carried out with water showed that the response of the measuring apparatus to the variations of hydraulic pressure was instantaneous [23–26].

It is important to note that pore pressure variations inside the mix significantly depend on the material's hydraulic conductivity. Fresh cement-based materials exhibit a lower hydraulic conductivity than pure granular materials [27]. Even if pore pressure variations are expected to be greater in the shearing zone for low-permeability materials such as cement-based materials, pressure variations can be partly absorbed through the sample (between the shearing zone and the measuring device at wall level). This implies that pore pressure variation amplitude is not an intrinsic parameter, but that it also depends on the device geometry.

2.3. Procedure

In the first part of the study self compacting cement paste (SCP), saturated sand and common industrial self-compacting concrete (SCC) were tested. Self compacting cement paste behavior is dominated by colloidal interaction, while saturated sand behavior is frictional. Comparison of test results in these two extreme cases advances our understanding of SCC shearing behavior.

In the second part, mortar mixes M_0 to M_3 (Table 1) were designed to evaluate pressure and yield stress evolutions as the sand fraction increases in the mix.

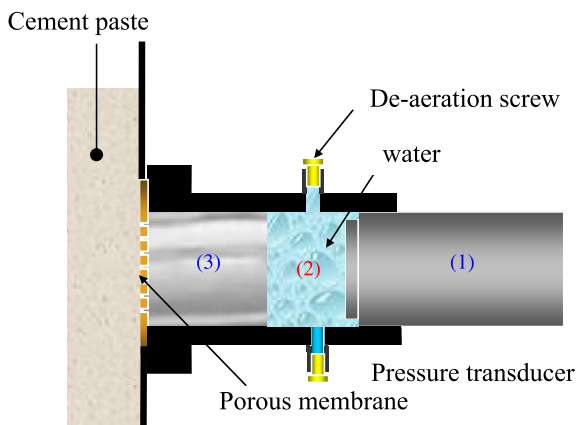


Fig. 2. Pore pressure measurement system – (1) pressure transducer – (2) de-aerator block – (3) filtering device.

The last two columns of Table 1 present tests performed on the samples. Saturated sand and SCC were directly tested in the home-made rheometer, whereas a study of the yield stress increase linked to thixotropy was carried out first on mortar mixes (with device 1).

2.3.1. Yield stress measurement (device 1)

Fresh cement-based material rheology is quite difficult to measure. These mixes exhibit time-dependent behavior due to thixotropy [1,28–32] and the beginning of hydration [33]. The thixotropic behavior of cement-based materials is related to the coagulation, dispersion, and re-coagulation of cement particles [29,31,34].

Yield stress is the most relevant parameter to study the impact of rheology on the common casting process [18–21]. However, as for any flocculating suspension, yield stress largely depends on the structural build-up of the colloidal cement suspension. As a result, the yield stress of cement-based materials increases at rest as the material is structured. As a result, an experimental protocol has to be found in order to take into account the structural build-up. Roussel predicts a linear increase of the yield stress over resting time. This relationship is written as follows in [35]:

$$\tau_0(t_{rest}) = \tau_0(0) + A_{thix} \cdot t_{rest} \quad (1)$$

where t_{rest} is the resting time and A_{thix} is the structuration rate of the cement-based material in Pa/s. As a result, it is crucial to link the yield stress to the material's resting time.

Just after mixing, some of the mortar was poured into a 20 cm × 20 cm × 5 cm container. A measurement stage was performed for 120 s on the Anton Paar rheometer, to obtain the yield stress at a given resting time, following the stress growth procedure described by Mahaut et al. [22]. A low constant shear rate is applied to the material (vane velocity 0.1 rpm). At such a low shear rate, viscosity effects are negligible and stress growth procedure makes it possible to work out the yield stress. Hackley and Ferraris [36] provide the yield stress standard definition as the critical stress below which the material behaves like a solid. Once the torque peak value is reached, the yield stress value can be determined, as the material flows in the sheared zone. In consequence, the yield stress is computed from the torque peak value as in [37]. It is considered that when the torque value is maximal, yield stress is reached on the sheared surface described by the vane rotation [38,39]. In consequence yield stress is written:

$$\tau_0 = \frac{C}{\frac{\pi D^2}{2} \cdot (H + \frac{D}{3})} \quad (2)$$

where C is the torque peak value, H and D are the tool height and diameter, respectively.

Every 10 min, the vane was moved in the sample to perform another measurement. The gap between each measurement location and the container wall was wide enough to avoid any scaling or wall slip effects (more than ten times the maximum particle diameter).

2.3.2. Torque and pressure measurement (device 2)

Just after mixing for self-compacting designs, or after 1 h for mortars, mixes were poured into the container of the pressure-fitted device to measure both pore pressure and torque once every 40 min until an age of about 3 h. The vane (120 mm height, 120 mm diameter) was immersed in the tested sample at a depth of 90 mm. This depth ensures that the pressure sensors face the middle of the vane. Vibrations were applied by a vibrating poker to ensure a total destructure of the suspension (cement particle dispersion). The poker diameter is 30 mm and was immersed between the vane and the container at a depth of 120 mm. The poker is moved inside the sample in order to vibrate the whole sample. This dynamic excitation breaks all the reversible bonds due to flocculation or hydration between cement particles. This vibration cancelled the yield stress increase of the material at rest, due to thixotropic behavior

[28]. The fluid suspension then underwent a stress growth test at a vane velocity of 0.6 rpm for a period of 150 s, and the pastes were allowed to rest for several minutes. The protocol and analysis of stress growth is described in the previous section. The procedure was renewed over 3 h. It should be noted that vibration was applied before but not during each stress growth. At rest and after vibration, the torque is null, and hydraulic pressure corresponds to the weight of the material above the sensor. Material homogeneity was checked after the test. No water bleeding or aggregates volume fraction gradient were observed.

3. Contraction and dilatancy phenomena during shearing: sand and self-compacting mixes

3.1. Sand

The French normalized sand, described in Table 1, was saturated, compacted with a drop hammer and subjected to vibrations. The measured solid volume fraction was 0.65. Fig. 3 shows the evolution of torque and pressure during shearing at a constant rotational velocity. An increase in torque occurs simultaneously with a drop in pore pressure during stress growth. Then, simultaneous peaks in torque and pore pressure are observed, followed by a return of pore pressure to its initial value, and a torque decrease to a constant value. This expected result is well described as the Reynold's dilatancy phenomenon [40].

In the pre-peak phase, the torque and the drop in pore pressure evolve simultaneously. The effective stress on a granular medium increases, and the frictional effect between particles is magnified. Consequently, the shear stress and the recorded torque increase while the vane rotates. At the tested solid fractions, shearing induces sand steric effects leading to dilatancy and a measured yield stress linked to the density and frictional characteristics of sand contact points. The pore volume increase induces a pore pressure decrease. It should be noted that the torque peak coincides with the minimal pore pressure.

After the peak, the torque decreases sharply and remains constant due to the frictional behavior of sand. Due to the high hydraulic conductivity of sand, water flows quickly through the sand, both porosity and pore pressure return toward the initial value. As expected, the final variation of pressure after shearing is null in saturated sand, as the water level has not changed after the test.

3.2. Self-compacting paste

In any study of SCP or SCC, it should be kept in mind that the behavior of cement-based material is time-dependent. At rest, during the 'dormant' period before the material begins to set, both reversible and irreversible bonds between cement particles are created [1,29,31,34]. This coagulation–flocculation mode induces a structural

build-up of the cement paste at rest which is known to induce a linear increase of the paste yield stress during the first hour. Then, the hydration rate of the cement increases. Setting begins, water is consumed and paste stiffness rapidly increases as does the hydrates solid volume fraction [24,41].

Fig. 4 shows an increase of pore water pressure between each shearing test during the first 100 min of the test. At this age, the cement paste flow regime is not frictional, contrariwise to saturated sand [2]. SCP behaves as a low yield stress fluid with a behavior dominated by cement particles colloidal interactions. This phenomenon can be explained as follows: at rest, particle clusters are formed in cement paste [29,31]. The bonds between particles can be reversible or irreversible, and are held to be responsible for the material's thixotropic behavior [2,29,31]. During shearing, the reversible bonds are broken, leading to a shrinkage effect inside the mix, and a reduction of the particle assembly volume in the sheared band [6]. This reduction of particle assembly volume induces a slight increase in pore pressure. When cement particles move, they can also meet other types of resistance (such as viscous resistance) from the surrounding cement particles [42]. After the peak, if the cement paste is allowed to rest, it is observed that the water pressure becomes hydrostatic again. We note that no significant torque was observed (Fig. 4), due to the torque sensor sensitivity and the SCP's low yield stress.

After 100 min, the energy of vibrations is no longer sufficient to break the bonds, due to thixotropy and the beginning of hydration. These new-formed bonds between particles seem to create a percolated network. The C–S–H have also adsorbed several layers of water molecules [43], which means that formed hydrates increase the solid volume fraction. At this stage, cement paste begins to behave as a dilative frictional material: shearing induces a decrease in pore water pressure. A solid cement particle network has been set, and dilatancy in the shearing band induces a suction effect on the whole network. Each torque peak occurs simultaneously with a drop in hydraulic pressure. Actually there is a competition between two phenomena:

1/At rest and after vibrations, pressure represents the apparent weight of the suspension. Then, as shown in Fig. 5, the pressure globally decreases over time: this is the effect of the increase of wall friction stress due to structural build-up. This result has already been observed in recent studies on formwork pressure evolution [44–48].

2/During shearing, a short time suction occurs when the granular medium is dilative. Fig. 5 is a zoom on one experimental increment. The observation of both torque and pressure curves leads to a few remarks:

- a peak in torque corresponds to a dramatic drop in pressure;
- after the stress peak, the torque is reduced and tends toward an equilibrium value while the rotation speed is kept constant [22];

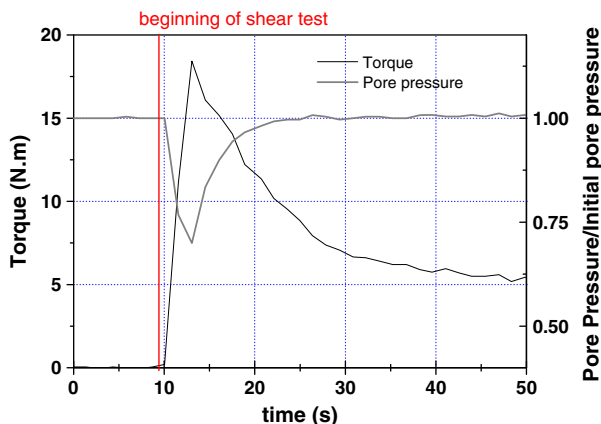


Fig. 3. Saturated sand Mortar test – torque and relative pore pressure variation for saturated sand.

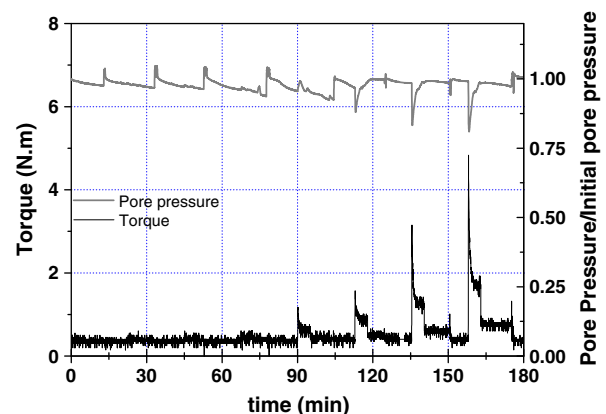


Fig. 4. Cement paste test – torque and relative pore pressure variation for cement paste at an early age.

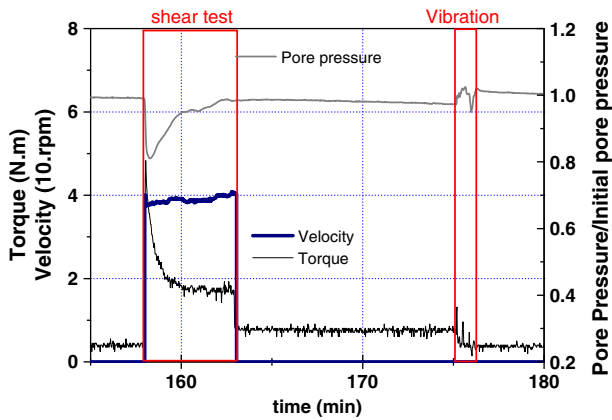


Fig. 5. Zoom on cement paste results while shearing.

- pressure stabilizes at a lower level than before shearing;
- after vibrations, torque is null and pressure returns to its pre-shearing level.

3.3. Self compacting concrete

SCC is described in Table 1. Until the age of 2 h, pressure measurements shown in Fig. 6 express no clear tendency, as the measurement values are indistinguishable from the “noise” produced during the test. This may confirm the competition between the two phenomena acting on pore pressure: dilatancy linked to the presence of an interconnected particle network inducing a drop in pressure, and the breakage of cement colloidal bonds leading to a smooth increase in pressure. For the tested SCC, a balance seems to appear between the two phenomena.

After 2 h, drops in pressure under shearing appear, showing that the suspension is beginning to behave like a saturated granular material due to the presence of a well-formed percolated particle network.

After 3 h and due to cement hydration, results are not reliable as the SCC is no longer saturated. This phenomenon was observed and well explained by Tchamba et al. [44]. Pore pressure decreases rapidly and irreversibly.

3.4. Summary of results on pore pressure variation during shearing

Several observations can be highlighted on the basis of these tests:

- Under shearing, after a given time period, the pore pressure varies slightly, positively for viscoelastic suspensions such as cement paste, and negatively for fluid-saturated granular suspensions such as saturated sand or cement-based mixes.

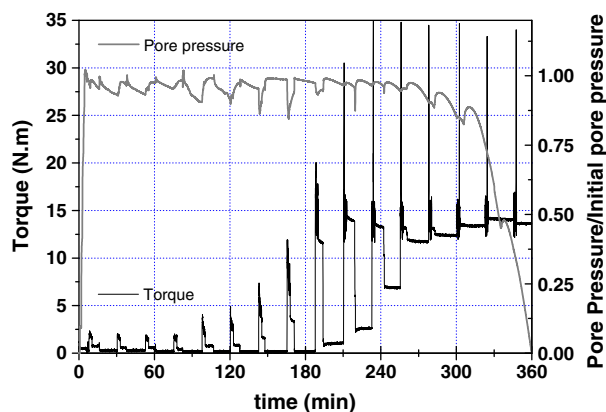


Fig. 6. Concrete test — torque and relative pore pressure variation for concrete at an early age.

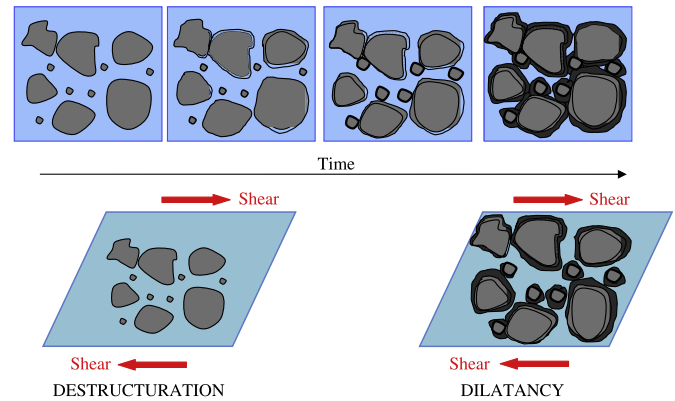


Fig. 7. Hydration process — effect of hydrate formation on the shearing properties.

- For a controlled rotation rate, optima in pore pressure and torque are recorded simultaneously.
- In granular suspensions, the equilibrium pressure is reached more rapidly for saturated sand than for SCC due to the difference in the medium's hydraulic conductivity [27].
- At some specific age for self-compacting cement-based materials, a drop in pore pressure occurs with yielding. This means that hydration evolves enough to create a percolation network between hydrated particles, as illustrated in Fig. 7. Before this specific age, shearing induces a deconstruction of the cement particles colloidal network, which leads to an increase in pore pressure.
- Pore pressure measurements can be efficient as long as the percolation due to hydration is not totally achieved and the media remains saturated (i.e. during the first 3 h, for the tested mixes).

The shearing behavior of the SCC seems to stand halfway between the saturated sand behavior and the cement paste behavior. However, results at this stage are too limited to draw conclusions. To go further, the influence of the aggregate content on the behavior of the cement mixes has to be analyzed.

4. Influence of sand content on pore pressure variation, yield stress, and thixotropy

Fig. 8 shows the evolution of the yield stress according to the sand volume fraction. As demonstrated by Yammine et al. [3] for SCC mix design, the rheological behavior of cement pastes containing aggregates may be governed by two kinds of aggregate interactions: hydrodynamic or frictional. The authors suggest that the second type of interaction appears when the aggregate solid volume fraction is sufficient to create a continuous contact network throughout the paste. For spherical particles, this contact network is reached for a critical volume fraction ϕ_c equal to $0.79\phi_m$, where ϕ_m is the close packing sand volume fraction. A value of 0.67 has been measured for ϕ_m on saturated normalized sand after compaction and vibration, leading to $\phi_c = 0.53$. Fig. 8 clearly shows that the effect of granular interaction appears when the sand volume fraction is close to ϕ_c . A sharp increase in the yield stress according to the sand volume fraction is noticed from this critical value ϕ_c .

The yield stress versus aggregate volume fraction curves can be divided into two parts:

1) If $\phi < \phi_c$, the aggregate interactions are hydrodynamic. In this case, the yield stress of the aggregate suspension is proportional to the cement paste yield stress. The recent models of Chateau et al. [49] or Ildefonse et al. [50] predict the paste yield stress according to the aggregate volume fraction as demonstrated by Mahaut et al. [22], or Toutou and Roussel [51].

2) If $\phi_c < \phi < \phi_m$, the suspension behavior is mainly governed by the granular interactions. The increase in yield stress is linked to the

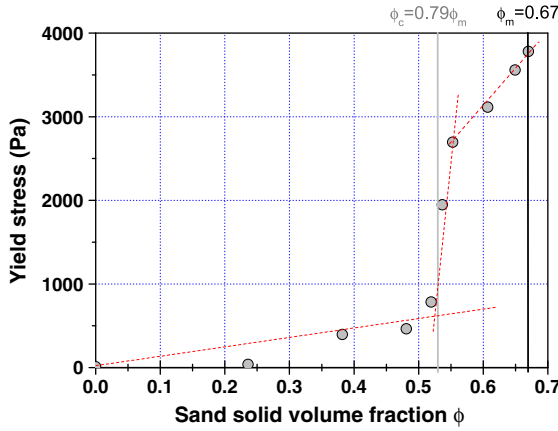


Fig. 8. Yield stress measured after 10 min of rest versus sand solid volume fraction. Tests are performed 10 min after the end of mixing.

increase in number of contacts between particles as the aggregate volume fraction increases, whatever the nature of the interstitial fluids. Two tests at $\phi = \phi_m$ for two suspending fluids, cement paste and water, were performed. The results (Fig. 9) show that the yield stress value evolution is similar. At the close packing volume fraction the interstitial fluid has no significant influence, and the yield stress is essentially controlled by granular interactions.

This change of behavior due to the aggregate volume content is expected to influence one of the most important characteristics of modern fresh concrete: thixotropy. Fig. 10 shows the evolution of non-dimensional yield stress (the ratio between yield stress and first measured yield stress value) of the paste at rest, over time, for four sand volume fractions. It appears that the Roussel assumption of a linear evolution of yield stress can be applied to the tested material during the first 45 min. At a low aggregate volume content (below ϕ_c), the material evolves at rest due to the reversible structuration of the cement paste's colloidal network. This setting has an important effect on the hydrodynamic interactions during shearing. In such a flow regime, Mahaut et al. [22] predict that the structuration rate A_{thix} introduced by Roussel [20] increases linearly with $\sqrt{(1-\phi)(1-\phi/\phi_{RLP})}^{-2.5\phi_{RLP}}$ where ϕ_{RLP} is the random loose packing volume fraction (measured at 0.56 for the sand after random filling of a known volume).

Fig. 11 compares the Mahaut model with experimental values, and shows that this modeling is not able to predict the structuration at rest when $\phi > \phi_c$. As shown in the figure, A_{thix} began to decrease when ϕ was greater than ϕ_c whereas modeled values predict an increase till the suspension reaches the random loose packing volume

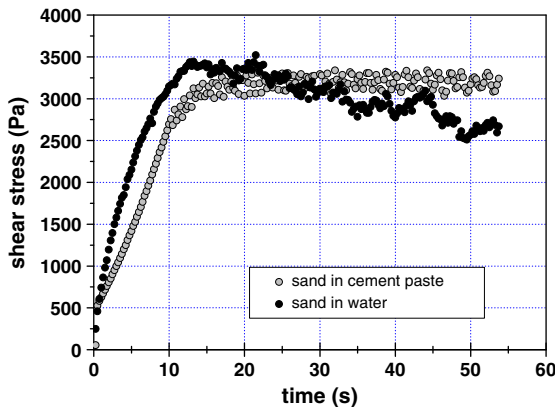


Fig. 9. Vane test results for suspensions of sand in water and in cement paste at a solid volume fraction of ϕ_m .

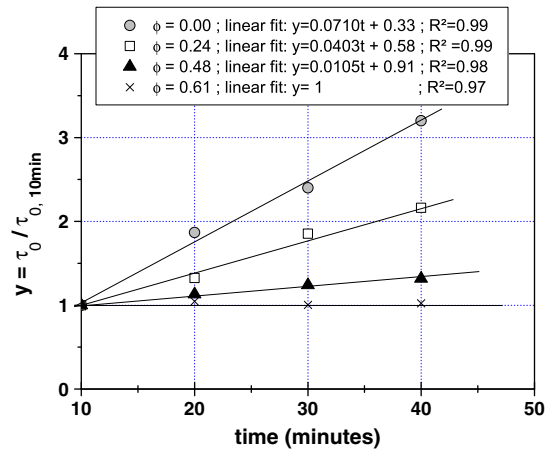


Fig. 10. Evolution of yield stress of the paste at rest as a function of time for four suspensions covering the range of tested sand volume fraction.

fraction of sand (where Mahaut modeling diverges). This shows that the structuration of the cement paste has less effect when an aggregates contact network already exists. Moreover, for the two highest-tested sand volume fractions, thixotropy can be neglected. This can be explained by the fact that the aggregates contact network is much stronger than the structuring colloidal network developed in the paste during the resting time.

This is well illustrated by Fig. 12. In this figure, the yield stress increase is shown by the ratio between the yield stress value at two arbitrary resting periods (10 and 40 min). Results show that this ratio decreases as the solid volume fraction increases, and converges toward 1 when ϕ tends to ϕ_m . This confirms that when a strong aggregates contact network exists, colloidal structuration can be neglected.

Common concrete mixes are designed for optimal granular assembly [52]. As a result, ϕ is close to ϕ_m and thixotropy has only a slight influence on the rheological behavior in comparison with SCC. Moreover, common concrete is subjected to vibrations to correctly fill the formwork. These vibrations break the reversible bonds between particles and limit the thixotropic effects linked to the cement paste. Nevertheless, it should be noted that common concrete presents a rheology which still and all depends on the paste rheology, as the addition of superplasticizer changes the concrete rheology without changing the paste volume. The extreme case would be the one presented on Fig. 9, where the aggregates' volume fraction is equal to ϕ_m . In this case, the aggregates volume fraction cannot be increased,

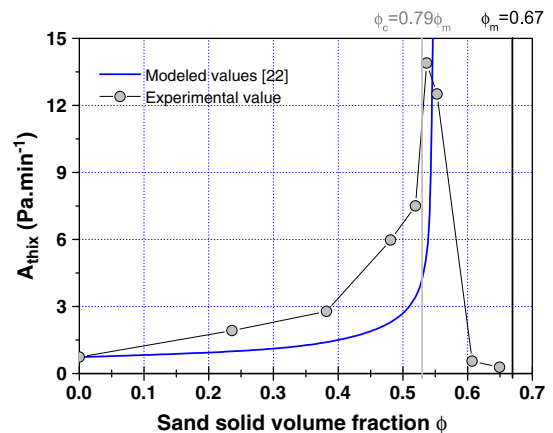


Fig. 11. Evolution of A_{thix} (Pa/min) for the studied mortars — resting period of 30 min (computed between 10 and 40 min after the end of mixing). Comparison between experimental measurements and modeled values [22].

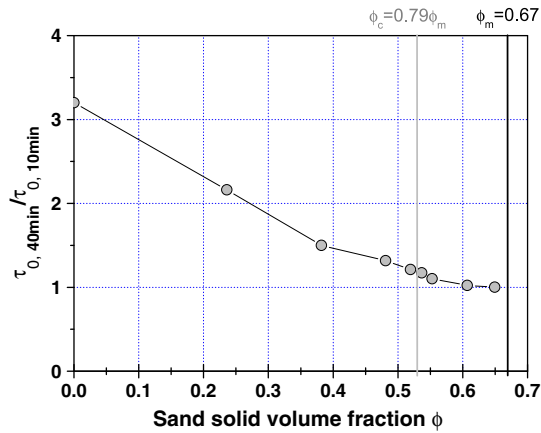


Fig. 12. Ratio between the yield stress after 40 min at rest and after 10 min (resting time starts just after the end of mixing).

and shearing properties are directly linked to the aggregates contact network. Indeed, thixotropy is crucial for modern concrete, such as SCC, which contains fewer aggregates in order to ensure flowability and granular stability [53,54]. This explains why the study of concrete thixotropy appears with the development of self-compacting concrete.

5. Correlation between the drop in pressure and the shear stress

As seen in part 3 for SCP and sand, recorded drops in pore pressure and maximum torque occur at almost the same time (Figs. 3 and 5). In this part of the study, the evolution of yield stress and variations of pore pressure are analyzed. The total variation ΔP in pore pressure equals the first maximum of pore pressures recorded during the shearing stage, minus the pore pressure at rest recorded before the corresponding shearing stage (Fig. 13). Overpressure corresponds to a positive ΔP while suction corresponds to a negative value.

Fig. 13 shows the evolution of yield stress and pore pressure versus sand volume fraction, for an age of 70 min. A drop in pressure occurs with the leap of yield stress observed if ϕ ranges between 0.53 and 0.56. These observations are consistent with the results of part 3: the paste becomes a “hard” suspension, governed by granular friction and no longer governed by colloidal interactions as described by Coussot and Ancey [2]. As a result particles must move in relation to each other to produce yielding. Thus dilatancy occurs, under a bigger inter-particulate force than for “soft” suspensions. Whenever there is cement percolation, cement paste can flow under less stress around

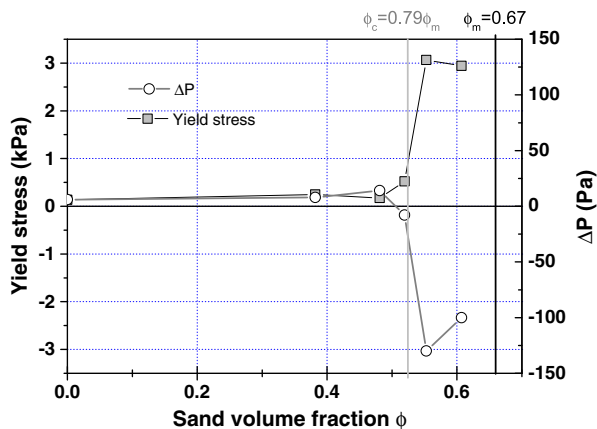


Fig. 13. Evolution of yield stress and variation in pore pressure ΔP versus Sand fraction (measurement performed at 30 min after the end of mixing).

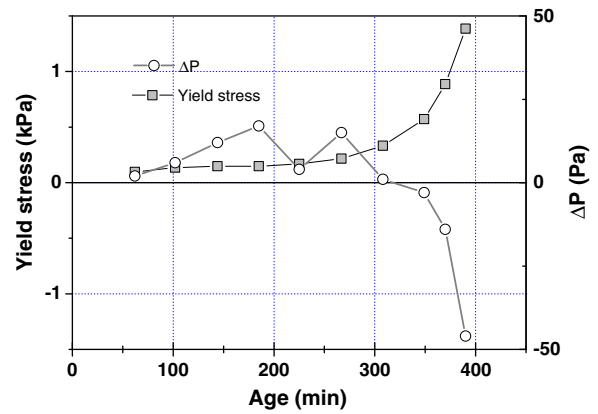


Fig. 14. Evolution of yield stress and variation in pore pressure ΔP with age, for the cement paste.

sand particles. Dilatancy, producing a suction in the sheared area (drop in pore pressure), becomes preponderant if ϕ is greater than 0.53. This value can be considered as the critical value ϕ_c defining the limit between “soft” suspensions and “hard” suspensions (aggregate contact network apparition).

Fig. 14 follows the evolution of the drop in pore pressure and yield stress versus the age of the cement paste. These two parameters vary symmetrically. After 300 min of hydration time, a drop in pressure and a yield stress increase are observed. Such shear behavior is similar to mortar behavior. Dilatancy probably occurs, meaning that solid hydrates present a sufficient solid fraction to percolate through the paste.

Figs. 13 and 14 clearly show that drops in pore pressure and increase in yield stress are correlated. To quantify the relationship between these parameters, the different points are drawn on a yield stress versus drop in pressure graph (Fig. 15). These points seem to be aligned, which clearly confirms that dilatancy-induced drops in pore pressure are linked to particle percolation and directly influence the yield stress value.

Considering the assembly of percolated wet particles, the shear strength is linked to both cohesion and inter-particle friction (Coulomb law). Husband et al. [55] have shown that non-colloidal particles present a yield stress linked to particle jamming.

Particle friction forces are largely considered proportional to normal stress. If particle percolation is reached, the particles are pushed together to form chains which change the stress distribution and increase the particle friction force [56]. Such chains create normal stresses acting on the shearing zone and increase particle friction [57–59]. This trend is observed in confined conditions for high solid-volume fractions, such as extruded mortars [60], where the internal friction angle is taken into account to describe the extrusion force.

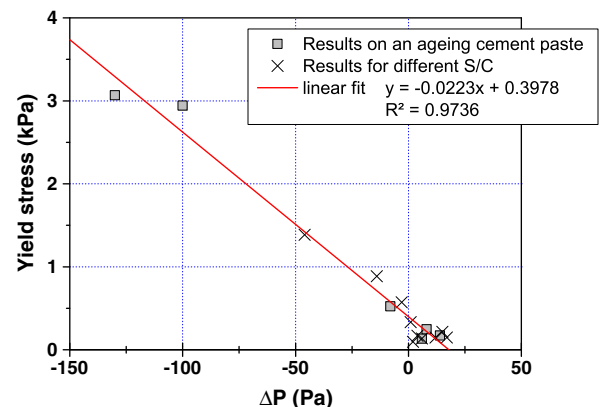


Fig. 15. Variation in pore pressure ΔP versus yield stress.

At this point, to produce a yield stress model for “hard” suspensions (i.e. for solid volume fractions over the critical solid volume fractions) inter-particle friction has to be considered.

6. Conclusions

An innovative rheometer set-up has been developed, to measure simultaneously torque and pore pressure changes at the container wall while shearing. These measurements provide crucial information on fresh mix behavior. The results clearly highlight two shear regimes according to the aggregate solid volume fraction ϕ in comparison to the critical solid volume fraction ϕ_c which corresponds to the percolation threshold of the suspension:

- below ϕ_c (i.e.: if $\phi < \phi_c$), the material's rheology is mainly governed by colloidal interactions. As a result, the yield stress increases over time, due to colloidal build-up. This means that thixotropy greatly influences the material's workability. Shearing induces a reduction of the recorded pressure which can be explained here by a breakage of the flocculated system. Such a low aggregate volume fraction corresponds to a self-compacting concrete mix design. This device could also help describe the hydration kinetics of cement mixes. When enough hydrates are formed, the solid percolation threshold is reached, and the mix starts to behave like a hard suspension as defined by Coussot and Ancey [9].
- beyond ϕ_c (i.e.: if $\phi \geq \phi_c$), the material's rheology is mainly governed by frictional aggregate interactions. As a result, the properties of the colloidal interstitial fluid have only a slight influence on the material's rheology. The material's yield stress does not evolve significantly over time. Granular-like behavior is clearly shown by the recorded drop in pore pressure, which is attributed to the dilatancy properties of the assembly over the percolation threshold.

These conclusions explain why the study of the thixotropy phenomenon becomes paramount with self-compacting concrete, as it induces changes in rheological behavior. Moreover, it highlights why thixotropy has become a key parameter in the 21st century, with the need to control casting or pre-casting processes when using modern self-compacting concretes.

Acknowledgments

The authors would like to acknowledge Y. Guevel, engineering assistant at the LIMATB, for his technical support in device control and data acquisition. They also wish to thank the European Community for its financial support through a state/region contract plan.

References

- [1] P.F.G. Banfill, The Rheology of Fresh Cement and Concrete – A Review, Proc. 11th International Cement Chemistry Congress, Durban, 2003.
- [2] P. Coussot, C. Ancey, Rheophysical classification of concentrated suspensions and granular pastes, *Phys. Rev. E* 59 (1998) 4445–4457.
- [3] J. Yammine, M. Chaouche, M. Guerin, M. Moranville, N. Roussel, From ordinary concrete to self compacting concrete: a transition between frictional and hydrostatic interactions, *Cem. Concr. Res.* 38 (2008) 890–896.
- [4] S. Mansoutre, P. Colombet, H. Van Damme, Water retention and granular rheological behavior of fresh C3S paste as a function of concentration, *Cem. Concr. Res.* 29 (1999) 1441–1453.
- [5] H. Van Damme Author, S. Mansoutre, P. Colombet, C. Lesaffre, D. Picart, Pastes: lubricated and cohesive granular media, *C. R. Physique* 3 (2002) 229–238.
- [6] N. Roussel, A. Lemaître, R.J. Flatt, P. Coussot, Steady state flow of cement suspensions: a micromechanical state of the art, *Cem. Concr. Res.* 40 (2010) 77–84.
- [7] N.E. Abriak, J.-F. Caron, Experimental study of shear in granular media, *Adv. Powder Technol.* 17 (2006) 297–318.
- [8] K.J.L. Stone, D. Muir Wood, Effects of dilatancy and particle size observed in model tests on sand, *Soils Found.* 32 (4) (1992) 43–57.
- [9] S. Amziane, C.F. Ferraris, SCC Evolution of formwork hydraulic pressure and of rheological properties, SP-233, in: Shi Caijun, Kamal H. Khayat (Eds.), *Workability of SCC: Roles of Its Constituents and Measurement Techniques*, SP of ACI, Spring Convention, New York (USA, 2006, p. 12.
- [10] S. Amziane, C.F. Ferraris, Cementitious paste setting using rheological and pressure measurements, *ACI Mater. J.* 104 (2) (2007) 137–145.
- [11] C.F. Ferraris, E. Koehler, S. Amziane, et al., Report on Measurements of Workability and Rheology of Fresh Concrete, , 2006 (70,pp., ACI 238.1R-08, ACI, USA).
- [12] P.F.G. Banfill, D. Beaupré, F. Chapedelaine, F. De Larrard, P. Domone, L. Nachbaur, T. Sedran, O.H. Wallevik, J.E. Wallevik, F. Ferraris, L.E. Brewer, Comparison of Concrete Rheometers: International Tests at LCPC (Nantes, France) in October, 2000 (Nistir 6819), National Institute of Standard and Technology (NIST, Gaithersburg, USA, 2001.
- [13] Q.D. Nguyen, D.V. Boger, Direct yield stress measurement with the vane method, *J. Rheol.* 29 (1985) 335–347.
- [14] N.J. Alderman, G.H. Meeten, J.D. Sherwood, Vane rheometry of bentonite gels, *J. Non-Newtonian Fluid Mech.* 39 (1991) 291–310.
- [15] V. Liddell Petra, D.V. Boger, Yield stress measurements with the vane, *J. Non-Newtonian Fluid Mech.* 63 (1996) 235–261.
- [16] P. Estelle, A. Perrot, C. Lanos, S. Amziane, Processing the vane shear flow data from Couette analogy, *Appl. Rheol.* 18 (2008) 34–43.
- [17] Y.L. Yeow, C.K. Woan, P.P.T. Pannie, Solving the inverse problem of Couette viscometry by Tikhonov regularization, *J. Rheol.* 44 (2000) 1335–1351.
- [18] N. Roussel, F. Cussigh, Distinct-layer casting of SCC: the mechanical consequences of thixotropy, *Cem. Concr. Res.* 38 (2008) 624–632.
- [19] N. Roussel, T.L.H. Nguyen, O. Yazoghli, P. Coussot, Passing ability of fresh concrete: a probabilistic approach, *Cem. Concr. Res.* 39 (2009) 227–232.
- [20] N. Roussel, A theoretical frame to study stability of fresh concrete, *RILEM Mater. Struct.* 39 (1) (2006) 81–91.
- [21] A. Yahia, K.H. Khayat, Analytical models for estimating yield stress of high-performance pseudoplastic grout, *Cem. Concr. Res.* 31 (2001) 731–738.
- [22] F. Mahaut, S. Mokkeddem, X. Chateau, N. Roussel, G. Ovarlez, Effect of coarse particle volume fraction on the yield stress and thixotropy of cementitious materials, *Cem. Concr. Res.* 38 (2008) 1276–1285.
- [23] N.R. Andriamanantsilavo, S. Amziane, Maturation of fresh cement paste within 1-to-10 m large formworks, *Cem. Concr. Res.* 34 (2004) 2141–2152.
- [24] S. Amziane, Setting time determination of cementitious material on measurements of the pore water pressure variations, *Cem. Concr. Res.* 36 (2) (2006) 295–304.
- [25] J. Assaad, K.H. Khayat, Variation of lateral and pore water pressure of self compacting concrete at early age, *ACI Mater. J.* 101 (4) (2004) 310–317.
- [26] J. Assaad, K.H. Khayat, H. Mesbah, Variation of formwork pressure with thixotropy of self compacting concrete, *ACI Mater. J.* 100 (1) (2003) 29–37.
- [27] V. Picandet, D. Rangeard, A. Perrot, T. Lecompte, Permeability measurement of fresh cement paste, *Cem. Concr. Res.* 41 (1) (2011) 330–338.
- [28] N. Roussel, Steady and transient flow behaviour of fresh cement pastes, *Cem. Concr. Res.* 35 (2005) 1656–1664.
- [29] J.E. Wallevik, Thixotropic investigation on cement paste: experimental and numerical approach, *J. Non-Newtonian Fluid Mech.* 132 (2005) 86–99.
- [30] R. Lapasin, A. Papo, S. Rajgeli, The phenomenology description of the thixotropic behavior of fresh cement pastes, *Rheol. Acta* 22 (1983) 410–416.
- [31] J.E. Wallevik, Rheological properties of cement paste: thixotropic behavior and structural breakdown, *Cem. Concr. Res.* 39 (2009) 14–29.
- [32] M.R. Geiker, M. Brandl, L.N. Thrane, D.H. Bager, O. Wallevik, The effect of measuring procedure on the apparent rheological properties of self-compacting concrete, *Cem. Concr. Res.* 32 (2002) 1791–1795.
- [33] P.F.G. Banfill, D.C. Saunders, On the viscosimetric examination of cement pastes, *Cem. Concr. Res.* 11 (1981) 363–370.
- [34] K. Hattori, K. Izumi, Rheology of fresh cement and concrete, in: P.F.G. Banfill (Ed.), *Rheology of Fresh Cement and Concrete*, Proc. Of International Conference organized by the British University of Liverpool, 16–29 March 1990, E & FN Spon, London, 1991, pp. 82–91.
- [35] N. Roussel, A thixotropy model for fresh fluid concretes: theory, validation and applications, *Cem. Concr. Res.* 36 (2006) 1797–1806.
- [36] V.A. Hackley, C.F. Ferraris, The use of nomenclature in dispersion science of technology, NIST Recommended Practice Guide N° 960–3, USA, 2001.
- [37] P.V. Liddell, D.V. Boger, Yield stress measurements with the vane, *J. Non-Newtonian Fluid Mech.* 63 (1996) 235–261.
- [38] J.M.P. Papenhuijzen, The role of particle interactions in the rheology of dispersed system, *Rheol. Acta* 11 (1972) 96–122.
- [39] M. Van den Tempel, Structure of multiphase systems, In: Houwink R, de Decker HK (eds) *Elasticity, plasticity and structure of matter*. Cambridge University Press, Cambridge, pp. 123–137.
- [40] O. Reynolds, *Phil. Mag.* Ser 5 (50) (1885) 469.
- [41] H. Sleiman, A. Perrot, S. Amziane, A new look at the measurement of cementitious paste setting by Vicat test, *Cem. Concr. Res.* 40 (2010) 681–686.
- [42] Z. Li, T.A. Ohkubo, Y. Tanigawa, Yield model of high fluidity concrete in fresh state, *J. Mater. Civil Eng.* (2004) 195–201.
- [43] M. Yang, C.M. Neubauer, H.M. Jennings, Interparticle potential and sedimentation behavior of cement suspensions, *Adv. Cem. Based Mater.* 5 (1997) 1–7.
- [44] J.C. Tchamba, S. Amziane, G. Ovarlez, N. Roussel, Lateral stress exerted by fresh cement paste on formwork: laboratory experiments, *Cem. Concr. Res.* 38 (2008) 459–466.
- [45] A. Perrot, S. Amziane, G. Ovarlez, N. Roussel, SCC formwork pressure: influence of steel rebars, *Cem. Concr. Res.* 39 (2009) 524–528.
- [46] S. Amziane, A. Perrot, T. Lecompte, A novel settling and structural build-up measurement method, *Measurement Science Technology* 19 (2008) 105–107.
- [47] G. Ovarlez, N. Roussel, A physical model for the prediction of lateral stress exerted by self-compacting concrete on formwork, *Mat. Struct.* 37 (2006) 269–279.
- [48] P. Billberg, From pressure generated by self-compacting concrete – influence of thixotropy and structural behaviour at rest, Ph.D Thesis, Department of Structural Engineering, The Royal Institute of Technology, Stockholm, 2006.

- [49] X. Chateau, G. Ovarlez, K.L. Trung, Homogenization approach to the behavior of suspensions of noncolloidal particles in yield stress fluids, *J. Rheol.* 52 (2008) 489–506.
- [50] B. Ildefonse, C. Allain, P. Coussot, Des grands écoulements naturels à la dynamique des tas de sable, Cemagref éditions, Paris, France, 2007.
- [51] Z. Toutou, N. Roussel, Multi scale experimental study of concrete rheology: from water scale to gravel scale, *Mat. Struct.* 37 (2006) 167–176.
- [52] F. de Larrard, Concrete Mixture Proportioning, E and FN Spon, London, 1999.
- [53] A.W. Saak, H. Jennings, S. Shah, New methodology for designing self-compacting concrete, *ACI Mater. J.* 98 (6) (2001) 429–439.
- [54] P.L. Domone, Self-compacting concrete: an analysis of 11 years of case studies, *Cement and Concrete Composites* 28 (2006) 197–208.
- [55] D.M. Husband, N. Askel, W. Gleissle, The existence of static yield stress in suspensions containing noncolloidal particles, *Journal of Rheology* 37 (1993) 215–235.
- [56] C.S. Campbell, Granular material flows — an overview, *Powder Tech.* 162 (2006) 208–229.
- [57] J.R. Melrose, R.C. Ball, “Contact networks” in continuously shear thickening colloids, *Journal of Rheology* 48 (5) (2004) 961–978.
- [58] R.S. Farr, J.R. Melrose, R.C. Ball, Kinetic theory of jamming hard-sphere startup flows, *Phys. Rev. E Stat. Phys. Plasmas Fluids Relat. Interdiscip. Topics* 55 (6 Suppl. B) (1996) 7203–7211.
- [59] A. Fall, A. Lemaître, F. Bertrand, D. Bonn, G. Ovarlez, Shear thickening and migration in granular suspensions, *Phys. Rev. Lett.* 105 (2010) (art. no. 268303).
- [60] A. Perrot, C. Lanos, P. Estellé, Y. Mélinge, Ram extrusion force for frictional plastic material: model prediction and application to cement paste, *Rheologica Acta* 45 (2006) 457–467.